

Code and constellation optimization for efficient noncoherent communication

Noah Jacobsen and Upamanyu Madhow
 Department of Electrical and Computer Engineering
 University of California, Santa Barbara
 Santa Barbara, CA 93106
 Email: {jacobsen,madhow}@ece.ucsb.edu

Abstract— We consider noncoherent communication techniques with large signal alphabets, where explicit (i.e. pilot symbol based) channel estimates are not required by the receiver, and iterative soft information exchange between noncoherent demodulator and channel decoder is employed for approaching Shannon-theoretic limits. Extrinsic Information Transfer (EXIT) functions are used to characterize convergence of the iterative receiver, enabling joint optimization of the inner modulation code constellation and symbol mapping with an outer binary channel code. We find that QAM constellations classically employed over the AWGN channel are inferior to modified constellation shapes based on aligned PSK rings with Gray-like amplitude/phase bit maps. EXIT analysis of turbo noncoherent communication further shows that standard convolutional codes are near optimal in serial concatenation with a unit-rate inner modulation code. The overall system is within 2.4 dB of Shannon capacity for the block fading channel at 1.8 bits/channel use, demonstrating that bandwidth-efficient noncoherent communication systems with reasonable complexity are now within reach.

I. INTRODUCTION

We consider the problem of bandwidth-efficient communication over time-varying channels with memory, such as those encountered in high data rate outdoor wireless mobile communication. We explore methods for the design and analysis of practical coded modulation schemes which approach the information-theoretic limits for such channels. Since it is unreasonable to assume that the receiver has prior knowledge of a time-varying channel, we consider *noncoherent* communication, in which the receiver must estimate both the channel and the data. While the design techniques developed here are quite general, we consider a block fading frequency-nonselctive channel model in our performance evaluations. This model allows for low-complexity noncoherent block demodulation techniques which implicitly estimate the channel gain and phase on each block, and is amenable to information-theoretic computations with which to compare the performance of practical coded modulation schemes. More importantly, however, the nonselective block fading model is an excellent approximation for existing and projected cellular systems. The slow variation of the channel gain is valid for any system in which the symbol rate is significantly larger than the Doppler frequency or residual frequency offset. Frequency nonselectivity applies, of course, to narrowband systems with bandwidth smaller than the channel coherence bandwidth, but it also applies to each subcarrier in wideband Orthogonal Frequency Division Multiplexed (OFDM) systems. Thus, in a typical OFDM system, the channel gain is well modeled as roughly constant over a time-frequency block of symbols whose size depends on the channel coherence time and coherence bandwidth.

The standard approach to transceiver design is to estimate the channel using pilots, and then to employ coherent demodulation assuming that the channel estimates are perfect. There are two main drawbacks of this approach: the overhead required for pilots to accurately track rapid channel variations is a significant fraction of the

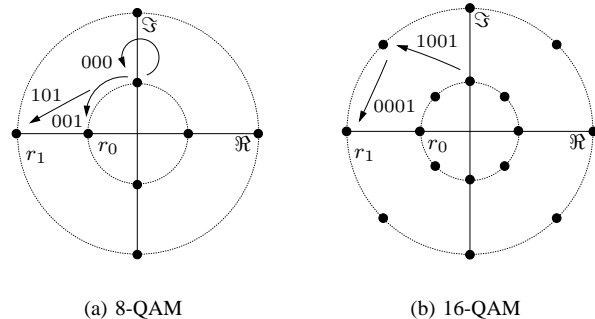


Fig. 1. Constellations based on aligned PSK rings with Gray-like symbol transitions are found to be well-suited for turbo noncoherent communication.

available bandwidth; and channel estimates based solely on the pilots are suboptimal, since they do not exploit the bulk of the transmitted energy, which is in the data. A number of recent papers [1], [2], [3], [4] consider the alternative of turbo noncoherent communication, with iterative joint estimation of the channel and data. We adopt the same basic transceiver architecture: an outer binary code, serially concatenated with a modulation code amenable to noncoherent demodulation. Specifically, the modulation code considered in our results is a simple generalization of standard differential modulation to QAM alphabets. No pilot symbols are employed. Iterative decoding with soft information exchange between the outer binary decoder and inner noncoherent block demodulator is employed.

A direct approach to Maximum Likelihood (ML) or Maximum A Posteriori (MAP) probability block noncoherent demodulation has complexity exponential in the block length. While recent results [5] have shown the surprising result that ML or MAP demodulation can be achieved with polynomial complexity, the methods in [5] are still too computationally demanding for typical applications, in contrast to the linear complexity of coherent demodulation. One approach to reducing the complexity is to implicitly estimate the channel gain jointly with the data, on a block by block basis. In past work on block noncoherent demodulation with PSK alphabets [4], [6], [7], this is accomplished simply by quantizing the channel phase into bins, in conjunction with a simple energy-based amplitude estimator. For a coded system as in [4], parallel coherent MAP decoders can be employed, one for each bin, followed by soft-combining of the outputs. However, the simple amplitude estimator in [4] does not work when the signal amplitude varies due to the use of Quadrature Amplitude Modulation (QAM) constellations. Furthermore, maintaining a large number of phase bins implies that the complexity of block noncoherent demodulation is still significantly larger than that

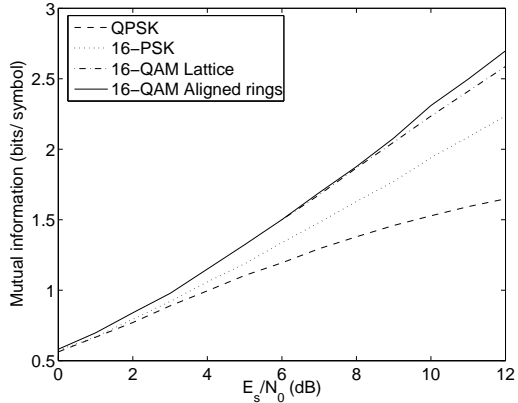


Fig. 2. 16-QAM constellations significantly improve the noncoherent mutual information for large-SNR.

of coherent demodulation. We provide an amplitude estimator that is bootstrapped with conventional two-symbol differential detection [8]. The estimate is computed only once per block, incurring only 0.4 dB loss compared to a *genie-based* system with perfectly known channel amplitude. The *bootstrap stage* also yields initial soft decisions to the outer decoder. As for the channel phase, we do quantize it as in [4], [6], [7], and run parallel MAP decoders, but in contrast to prior work, we employ a GLRT-based phase arbitration mechanism based on feedback from the outer decoder to reduce the number of phase bins to two after the first iteration. These simplifications are crucial to enabling efficient noncoherent communication with large QAM alphabets at complexity comparable to coherent systems.

Figure 2, computed using the techniques in [4], [9], shows the mutual information versus SNR for 16-ary constellations and QPSK. Evidently large constellations, and moreover, generalized amplitude/phase constellations are required to approach capacity at moderate to large SNR. The figure also reveals that mutual information is relatively insensitive to constellation shape for QAM constellations with a given number of signal points. For example, the mutual information of the lattice 16-QAM constellation and 16-QAM based on aligned PSK rings is approximately the same. We therefore need a tool other than Shannon theory for constellation and bit map design in coded noncoherent systems, and we turn to a modified form of EXIT analysis for this purpose.

Extrinsic Information Transfer (EXIT) charts [10], [11] are a popular means of obtaining insight into the behavior of systems with a turbo structure, given that they incur far less computational complexity than density evolution techniques [12]. A key tool for simplifying EXIT computations is a Gaussian approximation [11] for the information transferred back and forth between the decoder blocks within a turbo-like structure. One possible intuitive justification is the addition of many contributions in the log likelihood ratio (LLR) domain for a code with a long block length. We have modified this methodology to understand the behavior of noncoherent block demodulation, with iterative information exchange with an outer binary decoder. Since the demodulator has a relatively small block length, its output is not well approximated as Gaussian, and is therefore modeled in detail. However, the Gaussian approximation does apply to the output of the outer binary decoder, which operates on a large block length. The resulting EXIT technique allows us to characterize the performance of noncoherent block demodulation

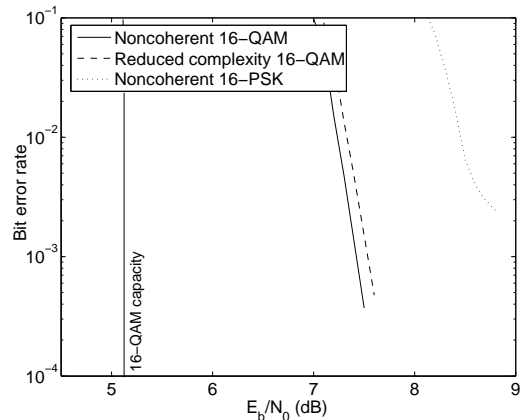


Fig. 3. Aligned rings 16-QAM realizes its capacity advantage at 1.8 bits/channel use.

for a given signal constellation and bit map, independent of the choice of the outer binary code. The results are employed to provide recommendations for 8-ary and 16-ary QAM constellations that are well matched to differential bit maps in phase and amplitude, depicted in Figure 1, as well as for the choice of outer binary channel code.

Example of a coded system: To illustrate the analysis of coded noncoherent communication with amplitude/phase constellations, consider the performance of aligned rings 16-QAM with unit-rate differential modulation and a rate-1/2 outer convolutional code, Figure 3. First, we note that the capacity advantage for 16-ary amplitude/phase constellations over 16-PSK at this rate is 1.6 dB. Since 1.2 dB gain is realized in the performance comparison, 0.4 dB may be attributed to increased sensitivity to amplitude distortion of amplitude/phase signaling. The 2.4 dB gap to capacity is understood with EXIT analysis, as follows: Derived from a folk theorem that the area under an EXIT chart equals the outer code rate [13], the modulation code bound (6) estimates the loss for employing unit-rate modulation in a serially concatenated structure as 1 dB. We further associate a 1 dB penalty for non-ideal channel coding by comparing the convergence threshold of the given code combination to the modulation code bound. Again, suboptimal demodulation of amplitude/phase constellations accounts for a 0.4 dB loss, and the conclusions of EXIT analysis are in agreement with simulation results.

II. NONCOHERENT TRANSCEIVER PROCESSING

In this section, we describe the channel model and turbo noncoherent communication with amplitude/phase constellations with complexity reducing techniques.

Channel model: A binary information sequence, \mathbf{U} , is mapped to codeword \mathbf{C} of the channel code, \mathcal{C} , and pseudo-randomly permuted to the code-bit symbol sequence $\tilde{\mathbf{C}}$. The cardinality of the modulation alphabet, \mathcal{A} , is M . Codewords in the modulation code, \mathcal{M} , belong in the T -fold product of the symbol alphabet, \mathcal{A}^T . In the *block fading model*, the channel is assumed to be constant over disjoint blocks of T symbol intervals, where T is the coherence length. Channel gains for different blocks are modeled as i.i.d. Thus, letting \mathbf{X} denote a block of T transmitted symbols, the block \mathbf{Y} of received symbols is given by

$$\mathbf{Y} = h\mathbf{X} + \mathbf{W}, \quad (1)$$

where the channel gain $h \triangleq ae^{j\theta}$ is a zero-mean, unit-variance proper complex Gaussian, written $h \sim \mathcal{CN}(0, 1)$. This is a classical Rayleigh fading model, with channel amplitude a Rayleigh, channel phase θ uniform over $[0, 2\pi]$, and a and θ independent. The additive noise vector, \mathbf{W} , is complex Gaussian, $\mathcal{CN}(0, 2\sigma^2\mathbf{I}_T)$, where \mathbf{I}_T stands for the $T \times T$ identity matrix.

Turbo noncoherent demodulation and decoding: The data, \mathbf{U} , and channel, $\{h\}$, are estimated jointly with turbo-like iterative demodulation and decoding of the received symbol sequence, $\{\mathbf{Y}\}$. Block-wise APP demodulation of differentially modulated channel data minimizes the uncoded symbol error rate. This is then used to compute extrinsic information regarding the outer code-bits to be passed back to the decoder. In practice, direct computation of the posterior probabilities of the transmitted symbols is infeasible, with complexity $O(M^T)$, scaling exponentially in the coherence interval. Following [4], [2], we consider an approximate MAP demodulator with channel amplitude estimation, and phase quantization with parallel coherent BCJR processing, details in [8]. The complexity is polynomial in M .

The noncoherent demodulator is comprised of parallel coherent demodulators, one for each quantized phase bin over the significant range of channel rotation (as defined by the rotationally invariant modulation code), and a channel amplitude estimator. The demodulator computes extrinsic *a posteriori* probabilities (APPs), $\Lambda_{\mathcal{M}}$, of the transmitted symbol sequence, based on the observed symbol sequence, $\{\mathbf{Y}\}$, and prior probabilities on the transmitted symbols, $\Pi_{\mathcal{M}}$. The channel decoder computes extrinsic code-bit probabilities, $\Lambda_{\mathcal{C}}$, with de-interleaved bit-wise APPs from the demodulator as priors, $\Pi_{\mathcal{C}}$. Decoder APPs are then re-interleaved and converted back to symbol priors for the next round of noncoherent demodulation. Random code-bit permutation justifies the independence of prior probabilities assumption of belief propagation decoding of concatenated codes. Demodulation and decoding are thus performed until a decoding success or satisfaction of complexity constraints.

Classical two-symbol maximum likelihood detection of differentially modulated data does not require channel knowledge and serves to bootstrap the receiver, providing (i) initial soft decisions to the outer channel decoder and (ii) symbol amplitude level probabilities to the channel amplitude estimator [8]. In our proposed *reduced-complexity* receiver, decoder computes extrinsic APPs based on bootstrap probabilities and sends them to the demodulator as priors. Next, noncoherent demodulation is performed with *all* phase branches, yielding conditional code symbol APPs for each phase branch. The GLRT criterion, described next, is then used to select the two phase branches producing the highest quality of soft information per block. Thus, only the first iteration of noncoherent demodulation considers all quantized phase bins, while subsequent iterations demodulate only the two selected phase bins. With these complexity reducing techniques the receiver requires approximately only twice as many demodulation computations as an idealized turbo-coded coherent system.

Phase selection: The method of phase quantization exhibits near capacity performance on the noncoherent block fading channel, yet each phase branch requires its own BCJR computation per iteration. We thus consider a criterion for ranking and pruning parallel phase branches as iterative demodulation and decoding are performed. We propose a Generalized Likelihood Ratio Test (GLRT) for phase branch selection, where the observation is the received signal and extrinsic information from the decoder, and the parameters to be estimated are the channel, h , and the transmitted data, \mathbf{X} . The GLRT operates with the joint likelihood function, $g_{x,q}(\gamma) \triangleq$

$f_{\Gamma|\mathbf{X},h}(\gamma|x, \hat{a} \exp(\phi q/Q))$, of the “observation” $\Gamma \triangleq \{\mathbf{Y}, \Pi\}$, given h and \mathbf{X} . GLRT based phase estimation involves maximization of the likelihood function first over transmitted symbol vectors and then over the quantized channel phase (2), viewed as joint maximum likelihood estimation of θ and \mathbf{X} based on the observation Γ ,

$$\hat{\theta}_{GLRT}(\gamma) = \arg \max_{q \in \mathcal{Q}} \max_{x \in \mathcal{M}} g_{x,q}(\gamma). \quad (2)$$

The inner maximization, referred to as the MLSE statistic, $g_{\hat{x},q} \triangleq \max_{x \in \mathcal{M}} g_{x,q}$, represents the weight of the Maximum Likelihood Sequence Estimate (MLSE) of the transmitted symbol vector on the q^{th} phase branch trellis. The MLSE statistic, typically computed with the Viterbi algorithm, is also computed by the forward recursion within the BCJR algorithm and is a natural choice for measuring the reliability of soft decisions output by each phase branch. Moreover, when used to choose the best two phase branches after the first receiver iteration, this metric yields a close approximation to the receiver that averages over all phase bins for all iterations, as shown in Figure 3.

III. EXIT FUNCTIONS OF NONCOHERENT CODES

We study the convergence behavior of iterative noncoherent demodulation and decoding via Extrinsic Information Transfer (EXIT) functions [10], [11]. The EXIT chart of a noncoherent code is a graphical description of iterative noncoherent demodulation and decoding, relating the mutual information of decoder messages communicated and code-bits estimated, as evolved through turbo-processing. Consider first the inner modulation code, \mathcal{M} , that maps code bits, $\tilde{\mathbf{C}} \triangleq \{C_n\}$, to channel symbols, \mathbf{X} . The noncoherent demodulator computes *a posteriori* probabilities, $\Lambda_{\mathcal{M}} = \{\Lambda_n\}$ defined with respect to the code-bits as LLRs,

$$\Lambda_n = \log \frac{Pr(C_n = 0|\Pi_{\mathcal{M}}, \{\mathbf{Y}\})}{Pr(C_n = 1|\Pi_{\mathcal{M}}, \{\mathbf{Y}\})} - \Pi_n, \quad (3)$$

where $\Pi_{\mathcal{M}} = \{\Pi_n\}$ denotes code-bit priors, $\Pi_n = \log \frac{Pr(C_n=0)}{Pr(C_n=1)}$. The *EXIT function*, A , for \mathcal{M} describes the mutual information of the code-bits and APPs, $a^{\text{out}} \triangleq I(\tilde{\mathbf{C}}; \Lambda_{\mathcal{M}})$, as a function of the *input* mutual information of the code bits and priors, $a^{\text{in}} \triangleq I(\tilde{\mathbf{C}}; \Pi_{\mathcal{M}})$, and channel SNR according to $a^{\text{out}} = A(a^{\text{in}}, SNR)$. Conditional probability density functions of decoder priors are often well-modeled as i.i.d., with a single-parameter family of Gaussian densities [11],

$$\Pi_n \sim \mathcal{N}(\pm 2\gamma, 4\gamma), \quad \gamma \in [0, \infty), \quad (4)$$

which has the interpretation of BPSK transmission of $\tilde{\mathbf{C}}$ over an AWGN channel at SNR γ . In this case, a^{in} has a simplified form, computed with an averaging estimate (5), see [11],

$$a^{\text{in}}(\gamma) = 1 - E[\log(1 - \exp(\Pi_n)) | C_n = 0]. \quad (5)$$

With \mathcal{M} discrete, we have $A : [0, 1] \rightarrow [0, 1]$, and the parameter γ is varied to generate a^{in} over the support of A . The *output* mutual information, a^{out} , is computed by measuring conditional probability density functions of Λ_n that are generated by the decoder fed with $\Pi_{\mathcal{M}}$ as in (4).

We next consider the EXIT function, B , of the outer channel code, \mathcal{C} . The APP decoder for \mathcal{C} computes its *a posteriori* probabilities of the code-bits, $\Lambda_{\mathcal{C}}$, with the priors $\Pi_{\mathcal{C}} = \text{perm}^{-1}(\Lambda_{\mathcal{M}})$ (permuted extrinsics from the demodulator). Letting $b^{\text{in}} \triangleq I(\mathbf{C}, \Pi_{\mathcal{C}})$ and $b^{\text{out}} \triangleq I(\mathbf{C}, \Lambda_{\mathcal{C}})$ denote input and output decoder mutual information, respectively, the decoder EXIT function is given by $b^{\text{out}} = B(b^{\text{in}})$. In many cases, log-APPs produced by the outer channel decoder, e.g. convolutional decoder, are well modeled as

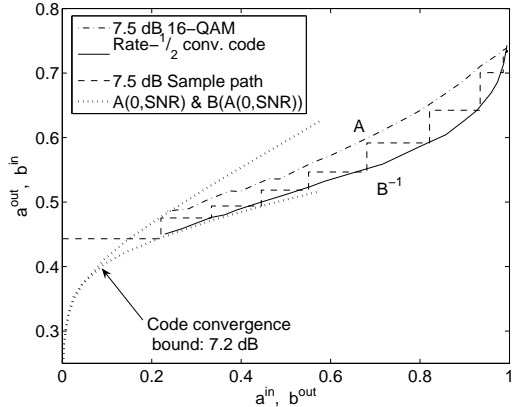


Fig. 4. EXIT chart of aligned rings 16-QAM (A) with convolutional outer code (B).

Gaussian. Then a^{out} is accurate when computed empirically from demodulator APPs, $\Lambda_{\mathcal{M}}$, resulting from the priors (4). However, we find that the extrinsic information, $\Lambda_{\mathcal{M}}$, produced by the demodulator is non-Gaussian, so that estimates of B based on Gaussian priors at the decoder do not accurately model density evolution for turbo noncoherent processing.

Since decoder priors are de-interleaved extrinsics from the demodulator, $\Pi_C = \text{perm}^{-1}(\Lambda_{\mathcal{M}})$, we propose the following approach for measuring decoder output mutual information, b^{out} . First, Gaussian code-bit priors are noncoherently demodulated; demodulator input mutual information, $a^{in}(\gamma)$, is computed with (5) and output mutual information, a^{out} , is estimated empirically. The resulting extrinsic code-bit APPs are then de-interleaved and sent to the decoder as priors, Π_C , now accurately modeling the priors observed in noncoherent processing. Decoder output mutual information is computed empirically from the resulting decoder extrinsics Λ_C .

Figure 4 is an EXIT chart of rate-1/2 convolutional code with aligned rings 16-QAM at an SNR of 7.5 dB (near the SNR threshold for this code combination) generated with the modified EXIT analysis. The inverse decoder transfer function, B^{-1} , is plotted since $b^{in} = a^{out}$. A sample path, corresponding to one channel realization and the resulting mutual information sequences, $\{a_k^{out}\}$, $\{b_k^{out}\}$, that arise from iterative noncoherent demodulation and decoding of a transmitted codeword is depicted.

We note some properties of EXIT charts and their implications:

Property 1: A given code combination is said to *converge* when $\lim_{k \rightarrow \infty} b_k^{out} = 1$, if and only if the information Bit Error Rate (BER) approaches zero. An equivalent condition for code convergence is that $B^{-1} < A$. In practice, we do not require the final decoder output mutual information to exactly equal one. In general, we have $B^{-1}(1) = 1$, and it may only be possible to arbitrarily approximate the convergence condition. However, a final decoder output mutual information less than one will give rise to an error floor.

Property 2: Channel SNR induces an ordering on demodulator EXIT functions such that if A and A' are measured at SNRs τ and τ' , with $\tau < \tau'$, then $A \leq A'$. The *convergence threshold* of a code is the SNR threshold, τ , for which the code converges if and only if $SNR > \tau$.

Property 3 (Conjecture): The area property of trellis decoders: $\int_0^1 B^{-1} = r_C$, where r_C denotes rate of the outer code. This property, proved only for erasures channels [13], has consistently

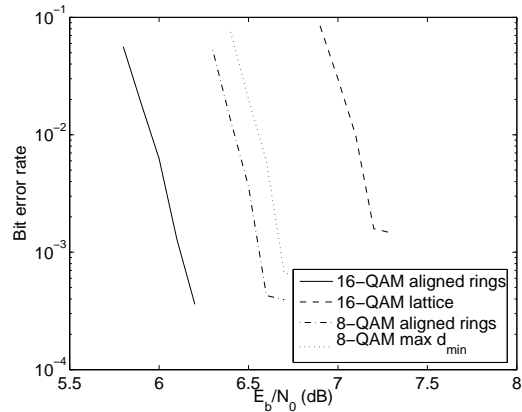


Fig. 5. Coded performance of various QAM constellations at 1.35 bits/channel use.

been observed in the literature, and in our own study, for a wide variety of channels. We show later that this property, if true, would imply that convolutional outer codes are near-optimal when the inner code is unit rate differential modulation.

As an empirical rule of thumb, average SNR does not affect the shape of the demodulator transfer function, B , but rather its offset. Since the channel decoder does not directly observe channel output, its transfer function is unaffected by SNR. These properties result in a quantitative framework for choosing or optimizing the modulation and channel codes and for developing reduced complexity receivers.

IV. CONSTELLATION DESIGN FOR NONCOHERENT COMMUNICATION

Gaussian input distributions, which are known to achieve unconstrained noncoherent capacity of the block fading channel [9], are more closely approximated by QAM constellations than PSK, especially for a large number of points. We first investigate noncoherent communication with lattice-based QAM constellations with differential Gray-like bit maps [8]. However, in simulations of a coded noncoherent system, we find that such lattice QAM constellations perform poorly, not delivering on the promised gains over PSK. We therefore consider an alternative class of QAM constellations, in the form of aligned PSK rings. These constellations, along with Gray-like bit maps for encoding data in the amplitude and phase transitions, are depicted in Figure 1. The ratio of ring radii and alignment angle are chosen to optimize noncoherent capacity. As discussed below, these constellations are found to perform much better than lattice-based QAM. We first observe that the noncoherent capacity is virtually identical for aligned rings and lattice QAM, and then turn to EXIT analysis for providing more precise guidance on constellation and bit map choice.

Figure 5 compares the simulated information BER of aligned PSK rings with lattice 16-QAM and (lattice-like) offset rings 8-QAM. Standard convolutional codes are employed for an overall data rate of 1.35 bits/channel symbol. The figure demonstrates the gain in using aligned rings over rectangular lattices: 2 dB for 16-ary constellations, and a less drastic 0.2 dB for 8-ary constellations. It also displays the advantage of constellation expansion with heavier coding: for the same information rate, 16-QAM aligned rings outperform 8-QAM aligned rings by 0.5 dB. Of course, this advantage is not realized for poor constellation and bit map choices: the lattice 16-QAM performs significantly worse than the 8-ary constellations at

the same information rate. EXIT charts explain this result: since the transfer function of the aligned rings constellation lies strictly above that of the corresponding lattice constellation, the convergence threshold with any outer code will be strictly larger for the lattice constellations.

Unit-rate rotationally-invariant differential modulation codes are well-suited to block noncoherent processing for their low-complexity demodulation and bootstrap functionality. We now quantify the performance penalty associated with this restriction (e.g., as opposed to using more sophisticated trellis-based modulation codes) for a serially concatenated system with an outer binary code. To this end, we invoke the conjectured area property, which states that the rate of the outer decoder equals the area under its exit curve, B^{-1} . The best possible (typically unrealizable) choice of outer code is when the decoder curve perfectly matches the inner demodulator curve at the convergence threshold. Thus, the highest possible rate of the outer code for convergence at a given SNR is the area under the demodulator curve at that SNR. This provides the following upper bound on the achievable rate (with serial concatenation) as a function of SNR for a given inner modulation code, as a function of its exit curve A :

$$I_{\mathcal{M}}(SNR) = \log_2(M) \frac{T-1}{T} \int A(u, SNR) du. \quad (6)$$

We term this bound the *modulation code bound*. Figure 11 compares the noncoherent capacity for aligned rings 16-QAM with the preceding upper bound on the achievable rate, using the same constellation, when restricted to using serial concatenation with a unit rate differentially modulated inner code with Gray-like bit maps.

V. CHANNEL CODING FOR NONCOHERENT MODULATION

We finally address the choice of outer channel codes, given a particular inner modulation code. In order to estimate the gap to the modulation code bound, $I_{\mathcal{M}}$, a lower bound on the SNR convergence threshold of a given channel code is obtained by appealing to the waterfall behavior of concatenated codes and considering the first iteration of demodulation and decoding as a function of channel SNR. By Property 1, a necessary condition for code convergence is that the first iteration produces a net increase in demodulator output mutual information, i.e. $a_0^{out} < a_1^{out}$. The *code convergence bound* (CCB) is defined as the smallest SNR for which this condition holds. Note that if the demodulator fails to yield a net increase in output mutual information in any one iteration, then the turbo demodulation and decoding algorithm has reached a fixed point solution, and no further increase (or decrease) in mutual information is possible. In general, the CCB will be tight, given the waterfall characteristic of turbo-processing. In Figure 4, the CCB corresponds to the SNR at which the dotted curves, $A(0, SNR)$ (upper) and $B(A(0, SNR))$ (lower, inverse plotted), diverge. For the standard rate-1/2 convolutional code employed, the bound is 7.2 dB.

In general we find that the EXIT function of a standard convolutional code is well-matched to unit-rate aligned-rings modulation codes. Optimization of the degree sequence of an irregular LDPC code for the specific context of noncoherent communication in block fading can potentially close the gap to the modulation code bound. On the other hand, we claim that standard convolutional codes are near-optimal for noncoherent differential amplitude/phase modulation. Taking the CCB as the threshold for the code combination in Figure 4 and comparing to $I_{\mathcal{M}}$, Figure 6, idealized channel coding could improve the convergence threshold by at most 1 dB. Since achieving the modulation code bound requires infinitely many demodulation

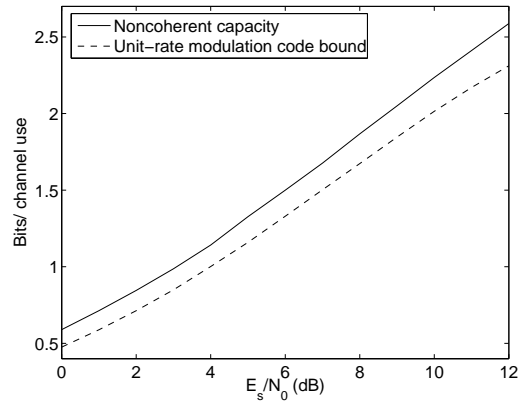


Fig. 6. The modulation code bound for unit rate differential modulation with 16-QAM aligned rings is about 1 dB away from the noncoherent capacity for that alphabet.

and decoding iterations (by definition the decoder transfer function is perfectly matched and coincident with the demodulator function), we conjecture that only 0.5 dB is gained by optimizing the channel code. Thus, we conclude that standard convolutional coding is near-optimal for a unit-rate differential modulation code.

REFERENCES

- [1] R.-R. Chen, D. Agrawal, and U. Madhow, "Noncoherent detection of factor-graph codes over fading channels," in *Proc. Conf. on Information Sciences and Systems (CISS)*, Princeton, NJ, USA, Mar. 2000.
- [2] M. Peleg, S. Shamai, and S. Galán, "Iterative decoding for coded noncoherent MPSK communications over phase-noisy AWGN channel," *IEEE Proc. Communications*, vol. 147, no. 2, pp. 87–95, Apr. 2000.
- [3] P. Hoehner and J. Lodge, "Turbo DPSK: Iterative differential PSK demodulation and channel decoding," *IEEE Trans. Communications*, vol. 47, no. 6, pp. 837–842, June 1999.
- [4] R.-R. Chen, R. Koetter, D. Agrawal, and U. Madhow, "Joint demodulation and decoding for the noncoherent block fading channel: a practical framework for approaching channel capacity," *IEEE Trans. Communications*, vol. 51, no. 10, pp. 1676–1689, Oct. 2003.
- [5] I. Motedayen-Aval and A. Anastasopoulos, "Polynomial-complexity noncoherent symbol-by-symbol detection with application to adaptive iterative decoding of turbo-like codes," *IEEE Trans. Communications*, vol. 51, no. 2, pp. 197–207, Feb. 2003.
- [6] D. Warrier and U. Madhow, "Spectrally efficient noncoherent communication," *IEEE Trans. Information Theory*, vol. 48, no. 3, pp. 651–668, Mar. 2002.
- [7] O. Macchi and L. Scharf, "A dynamic programming algorithm for phase estimation and data decoding on random phase channels," *IEEE Trans. Information Theory*, Sept. 1981.
- [8] N. Jacobsen and U. Madhow, "Reduced-complexity noncoherent communication with differential QAM and iterative receiver processing," in *Proc. Conf. on Information Sciences and Systems (CISS)*, Baltimore, MD, USA, Mar. 2003.
- [9] T. Marzetta and B. Hochwald, "Capacity of a mobile multiple-antenna communication link in Rayleigh flat fading," *IEEE Trans. Information Theory*, vol. 45, no. 1, pp. 139–157, Jan. 1999.
- [10] S. ten Brink, "Convergence behavior of iteratively decoded parallel concatenated codes," *IEEE Trans. Communications*, vol. 49, no. 10, pp. 1727–1737, Oct. 2001.
- [11] M. Tüchler and J. Hagenauer, "EXIT charts of irregular codes," in *Proc. Conf. on Information Sciences and Systems (CISS)*, Princeton, NJ, USA, Mar. 2002.
- [12] T. Richardson and R. Urbanke, "The capacity of low-density parity-check codes under message-passing decoding," *IEEE Trans. Information Theory*, vol. 47, no. 2, pp. 599–618, Feb. 2001.
- [13] A. Ashikhmin, G. Kramer, and S. ten Brink, "Extrinsic information transfer functions: model and erasure channel properties," *IEEE Trans. Information Theory*, to appear.